Iterative Interference Cancellation in FBMC-QAM Systems

Sumaila Mahama†, Yahya J. Harbi‡, Alister G. Burr†, and David Grace†
†Dept of Electronic Engineering, University of York, York, UK
‡University of Kufa, Najaf, Iraq
†{sumaila.mahama, alister.burr, david.grace}@york.ac.uk, ‡yahyaj.harbi@uokufa.edu.iq

***Abstract*—In this paper, we evaluate iterative interference cancellation (IIC) as a method to remove the intrinsic interference terms in filter bank multicarrier - quadrature amplitude modulation (FBMC-QAM) systems. We propose an IIC receiver that separates the received signal into even- and odd-numbered subcarrier components and use the demodulated even- and odd-numbered subcarrier symbols to iteratively remove the effect of interference. Numerical results show that the out-of-band emission performance of the IIC FBMC-QAM system is superior to that of OFDM and conventional FBMC-QAM. Bit error rate (BER) simulation results also indicate that the proposed IIC FBMC-QAM can effectively improve BER performance under different time-varying channels.**

***Index Terms*—Waveforms, 5G, OFDM, FBMC-QAM, iterative interference cancellation.**

I. Introduction

Current cellular networks, such as Long Term Evolution (LTE) and LTE-Advanced, adopt orthogonal frequency division multiplexing (OFDM) as the waveform for the air interface. However, OFDM is characterized by highly coordinated and synchronous transmissions, resulting in a high level of control overhead in the nework. With applications such as Internet of Things (IoT), the number of wireless devices is expected to grow exponentially over the next few years [1]. Hence, strict synchronization and coordination will require an exteremely large amount of control information. Also, most of these IoT applications will require asynchronous and low latency transmissions. To satisfy this surge in the number of connected devices, and the resulting increase in the amount of data handled by the network, 5G and beyond neworks will need to be highly versitile and adaptable [2]–[4].

For the first release of 5G, 3GPP has opted for a modified version of OFDM, mainly due to its backward compatibility with the existing 4G network [5]. However, in order to support asynchronous and uncoordinated transmission in future communications networks, the new air interface must address the strict synchronization and orthogonality constraints of OFDM-based waveforms. To this end, alternative waveforms, such filter bank multicarrier (FBMC), have been proposed in the literature to combat some of the shortfalls of OFDM [6]–[10]. FBMC employs a more advanced prototype filter, instead of the rectangular pulse shape filter used in OFDM, resulting in improved frequency localization. In addition, FBMC improves spectral efficiency, compared to OFDM, by removing the cyclic prefix (CP). Offset quadrature amplitude modulation (OQAM), which modulates subcarriers by transmitting the in-phase and quadrature samples with a shift of half the symbol period between them, has been adopted for FBMC in the literature. FBMC-OQAM achieves orthogonality in the real domain, with the imaginary part of the signal serving as intrinsic interference. The presence of intrinsic interference is a key drawback in FBMC-OQAM when adopted for MIMO applications. Furthermore, in the presence of multipath fading channels, the real orthogonality of FBMC-OQAM may be lost, resulting in intersymbol interference (ISI) and intercarrier interference (ICI). The use of equalization and interference cancellation has been proposed in the literature to eliminate ISI and ICI [11], [12]. In [13], the authors proposed an iterative interference cancellation (IIC) receiver to reduce ISI and ICI in SISO FBMC-OQAM systems. They extended their work to a MIMO-IIC approach with linear and successive interference cancellation (SIC) to reduce ISI and ICI in both MIMO-OFDM and MIMO-FBMC/OQAM systems in [14].

Recently, the use of complex valued QAM symbols instead of OQAM has been proposed in [15]. In [15], two different prototype filters were used for even- and odd-numbered subcarriers in order to achieve orthogonality and to remove the ISI and ICI terms. To further reduce the influence of residual interference in [15], [16] studied a channel estimation method based on an IIC algorithm. However, the proposed systems have a higher out-of-band (OOB) emission compared to OFDM and FBMC-OQAM due to the structure of the prototype filters. The authors in [17] proposed an interference-free FBMC system, which retains the better spectral confinement of FBMC systems by transmitting information on only even-numbered subcarriers to avoid ICI.

In this paper, we propose an IIC receiver to iteratively cancel the ISI and ICI inherent in FBMC-QAM systems. The approach is to separate the received signal into even- and odd-numbered subcarrier components and use the demodulated even- and odd-numbered subcarrier symbols to iteratively remove the effect of interference. The proposed system can achieve better OOB emission while making maximum use of the available frequency resources. This also enables application of some conventional MIMO techniques in FIMC systems. The excellent spectral confinement will also improve robustness for asynchronous transmissions.

The work described in this paper was funded by the European Commission under Project ID 722788 SPOTLIGHT.

The rest of the paper is organized as follows: Section II describes the FBMC-QAM system model. Section III outlines the proposed iterative interference cancellation algorithm for FBMC-QAM. Numerical results are presented in Section IV. Section VI concludes the paper.

II. FBMC-QAM SYSTEM MODEL

At the FBMC-QAM transmitter, the QAM symbols are separated into even- and odd-numbered subcarrier symbols. Each set of symbols then goes through an inverse fast Fourier transform (IFFT) block. The output of the $M/2$-IFFT of the data at the m-th even-numbered subcarrier of the n-th symbol is given as

$$b_{m,n}^{even} = \sum_{m=0}^{M/2-1} a_{m,n}^{even} e^{j\frac{2\pi}{M/2}mn} \tag{1}$$

where $a_{m,n}^{even} = a_{2m,n}^{even}$ $m \in \{0, 1, \dots M/2\}$ represent the even-numbered subcarrier symbols, and M is the total number of subcarriers. The vector form of $b_{m,n}^{even}$ for $m \in \{0, 1, \dots M/2\}$ is obtained as

$$\mathbf{b}_n^{even} = \mathbf{\Phi}\mathbf{a}_n^{even} \tag{2}$$

where $\mathbf{b}_n^{even} \triangleq [b_{0,n}^{even}, \dots, b_{M/2-1,n}^{even}]$, $\mathbf{a}_n^{even} \triangleq [a_{0,n}^{even}, \dots, a_{M/2-1,n}^{even}]$ and $\mathbf{\Phi}$ is the $M \times M/2$ IDFT matrix whose entry on the i-th row and j-th column is $e^{j\frac{2\pi ij}{M/2}}$. Similarly, the vector form of $M/2$-IFFT of the n-th odd-numbered sub-carrier symbol is given as

$$\mathbf{b}_n^{odd} = \mathbf{\Phi}\mathbf{a}_n^{odd} \tag{3}$$

The IFFT outputs are then multiplied by the prototype filter, i.e.

$$x_{m,n}^{even} = \sum_{k=0}^{2K-1} g[kM/2] b_{m,n-k}^{even} \tag{4}$$

where $g[i]$ is the prototype filter with overlapping factor K. In vector form, the transmit signal for even-numbered subcarrier symbols can be expressed as

$$\mathbf{x}_n^{even} = \mathbf{G}_n\mathbf{b}_n^{even} = \mathbf{G}_n\mathbf{\Phi}\mathbf{a}_n^{even} \tag{5}$$

where $\mathbf{x}_n^{even} \triangleq [x_{0,n}^{even}, \dots, x_{M/2-1,n}^{even}]$ and $\mathbf{G}_n$ is a matrix whose i-th row and j-th column is given as [17]

$$[\mathbf{G}_n]_{ij} = \begin{cases} g[(i-j)M/2], & \text{for } 0 \le i-j < 2K \\ 0, & \text{otherwise} \end{cases} \tag{6}$$

where $[\mathbf{P}_n]_{ij}$ represents the entry in the i-th row and j-th column of a matrix $\mathbf{P}$.

Unlike [15], which uses two different prototype filters for even and odd-numbered subcarrier, we employ the same prototype filter for both even and odd-numbered subcarriers. Hence, the transmit signal for odd-numbered subcarriers can be expressed as

$$\mathbf{x}_n^{odd} = \mathbf{G}_n\mathbf{b}_n^{odd} = \mathbf{G}_n\mathbf{\Phi}\mathbf{a}_n^{odd} \tag{7}$$

Hence, we have the discrete-time transmit signal during the n-th time slot as

$$\mathbf{x}_n = \mathbf{x}_n^{even} + \mathbf{x}_n^{odd} = \mathbf{G}_n\mathbf{\Phi}\mathbf{a}_n^{even} + \mathbf{G}_n\mathbf{\Phi}\mathbf{a}_n^{odd} \tag{8}$$

At the FBMC receiver, each symbol is filtered by the prototype filter. The receiver filter is designed to be the complex conjugate of the transmit filter [18]. The filter output is therefore given by

$$y_{m,n} = \sum_{k=0}^{2K-1} g^*[kM/2] x_{m,n}^{even} + \sum_{k=0}^{2K-1} g^*[kM/2] x_{m,n}^{odd} \tag{9}$$

where $\{\cdot\}^*$ denotes the complex conjugate. This is given in vector form as

$$\mathbf{y}_n = \mathbf{G}_n^H\mathbf{x}_n^{even} + \mathbf{G}_n^H\mathbf{x}_n^{odd} \tag{10}$$

$$= \mathbf{y}_n^{even} + \mathbf{y}_n^{odd} \tag{11}$$

where $\mathbf{y}_n^{even} \triangleq [y_{0,n}^{even}, \dots, y_{M/2-1,n}^{even}]$, $\mathbf{y}_n^{odd} \triangleq [y_{0,n}^{odd}, \dots, y_{M/2-1,n}^{odd}]$ and $\{\cdot\}^H$ denotes the Hermitian operator. The output of the $M/2$-FFT can be expressed as

$$\hat{b}_{m,n} = \sum_{m=0}^{M/2-1} e^{-j\frac{2\pi}{M/2}mn} y_{m,n} \tag{12}$$

The vector form of the FFT output can be written as

$$\hat{\mathbf{b}}_n = \mathbf{\Phi}^H\mathbf{y}_n \tag{13}$$

$$= \mathbf{Q}\mathbf{a}_n^{even} + \mathbf{Q}\mathbf{a}_n^{odd} \tag{14}$$

$$= \hat{\mathbf{b}}_n^{even} + \hat{\mathbf{b}}_n^{odd} \tag{15}$$

where $\hat{\mathbf{b}}_n^{even} \triangleq [\hat{b}_{0,n}^{even}, \dots, \hat{b}_{M/2-1,n}^{even}]$, $\hat{\mathbf{b}}_n^{odd} \triangleq [\hat{b}_{0,n}^{odd}, \dots, \hat{b}_{M/2-1,n}^{odd}]$ and $\mathbf{Q} = \mathbf{\Phi}^H\mathbf{G}_n^H\mathbf{G}_n\mathbf{\Phi}$.

In the presence of multipath channels and complex Gaussian noise, (13) can be rewritten as

$$\hat{\mathbf{b}}_n = \mathbf{H}\mathbf{Q}\mathbf{a}_n^{even} + \mathbf{H}\mathbf{Q}\mathbf{a}_n^{odd} + \tilde{\mathbf{z}}_n \tag{16}$$

where

$$[\mathbf{H}]_{p,q} = \begin{cases} h[(p-q)], & \text{for } 0 \le p-q < L, \\ 0, & \text{otherwise} \end{cases} \tag{17}$$

h is the multipath channel impulse response, $\tilde{\mathbf{z}} = \mathbf{\Phi}^H\mathbf{G}_n^H\mathbf{z}_n$, $\mathbf{z}_n \triangleq [z_{0,n}, \dots, z_{M/2-1,n}]$ is the vector form of the additive white complex Gaussian noise and L is the length of the channel impulse response.

In FBMC systems, the prototype filters are well-localized in the frequency domain. As a result the data on even-numbered (odd-numbered) subcarriers do not cause any interference with other even-numbered (odd-numbered) subcarrier symbols. Therefore, the demodulated signal of the n-th even-numbered subcarrier symbol is given by

$$\hat{\mathbf{a}}_n^{even} = \mathbf{H}_D\mathbf{a}_n^{even} + \underbrace{\mathbf{H}_{ISI}(\mathbf{Q}-\mathbf{I})\mathbf{a}_{n-1}^{even}}_{I_{ISI}^{even}} + \underbrace{\mathbf{H}_{ICI}\mathbf{Q}\mathbf{a}_n^{odd}}_{I_{ICI}^{odd}} + \tilde{\mathbf{z}} \tag{18}$$

Similarly, the demodulated signal of the n-th odd-numbered subcarrier symbol can be expressed as

$$\hat{\mathbf{a}}_n^{odd} = \mathbf{H}_D \mathbf{a}_n^{odd} + \underbrace{\mathbf{H}_{ISI}(\mathbf{Q}-\mathbf{I})\mathbf{a}_{n-1}^{odd}}_{I_{ISI}^{odd}} + \underbrace{\mathbf{H}_{ICI}\mathbf{Q}\mathbf{a}_n^{even}}_{I_{ICI}^{even}} + \tilde{\mathbf{z}} \tag{19}$$

where I_{ISI}^{even} and I_{ICI}^{odd} represent the ISI and ICI experienced by even-numbered sub-carrier symbols, I_{ISI}^{odd} and I_{ICI}^{even} are the ISI and ICI experienced by odd-numbered sub-carrier symbols. $\mathbf{H}_D$, $\mathbf{H}_{ICI}$, and $\mathbf{H}_{ISI}$ correspond respectively to the desired channel, the undesired channel that result in ICI and the channel from the previously decoded symbols that lead to ISI, and $\mathbf{I}$ is the identity matrix.

III. Iterative Interference Cancellation for FBMC-QAM

Due to the loss of complex orthogonality in FBMC-QAM, there is a high level of intrinsic interference as shown in (18) and (19). To reduce the level of intrinsic interference and improve the bit error rate (BER) performance, the undesirable terms must be removed from (18) and (19). In this work, we propose the use of an IIC algorithm to remove these interfering terms [13]. First, the receiver estimates the multipath channel responses $\mathbf{H}_{ICI}$, and $\mathbf{H}_{ISI}$. Then the matrix $\mathbf{Q}$ is computed using the filter response matrix $\mathbf{G}_n$ and IDFT matrix $\mathbf{\Phi}$. Next, using the current and previous values of the demodulated even- and odd-numbered subcarrier symbols, the receiver can evaluate I_{ISI}^{even}, I_{ICI}^{odd}, I_{ISI}^{odd} and I_{ICI}^{even} as shown in (18) and (19). Finally, the receiver can subtract the interference terms from the even- and odd-numbered data symbols, as shown in Fig. 1. This process is repeated iteratively until a predefined number of iterations is satisfied. Algorithm 1 shows the proposed IIC procedure in pseudo code.

Since FBMC systems use no cyclic prefix (CP), the interference channel matrix $\mathbf{H}_{ICI} = \mathbf{H}_{ISI} = \mathbf{H}_j \in \mathbb{C}^{N\times N}$ and can be expressed as

$$\mathbf{H}_j = \begin{bmatrix} 0_{E\times(N-E)} & \mathbf{H}_1 \\ 0_{(N-E)\times(N-E)} & 0_{(N-E)\times E} \end{bmatrix} \tag{20}$$

where $\mathbf{H}_1 \in \mathbb{C}^{E\times E}$, with $E = L-1$, is given by

$$\mathbf{H}_1 = \begin{bmatrix} h_{L-1} & \dots & \dots & h_0 \\ 0 & \ddots & & \vdots \\ \vdots & \ddots & \ddots & \vdots \\ 0 & \dots & 0 & h_{L-1} \end{bmatrix} \tag{21}$$

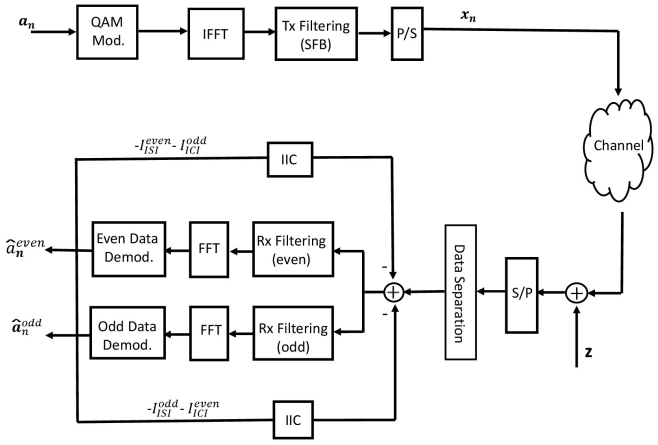

Fig. 1. Proposed FBMC-QAM IIC Transceiver

TABLE I
Simulation Parameters

Parameter	Specification
Filter	PHYDYAS prototype filter [8]
Overlapping factor (K)	4
Channel Bandwidth	5 MHz
Total number of Subcarriers	128
Number of resource blocks (RBs)	6
Number of Subcarriers per RBs	12
Subcarriers spacing	15 KHz
Number of slots per RBs	2
Number of symbols per slot	7
Modulation	4-QAM, 16-QAM
Number of IIC iterations	0, 1, 2, 3, 5
LTE Channel model	EVA, ETU

Algorithm 1 IIC Algorithm

Specify the maximum number of iterations I_{max}
Initialize number of iterations $i = 0$
while $i \leq I_{max}$ **do**
  Compute $\mathbf{H}_{ICI}$ and $\mathbf{H}_{ISI}$ from (20).
  Compute $\mathbf{Q}$ using $\mathbf{G}_n$ and $\mathbf{\Phi}$.
  Estimate I_{ISI}^{even}, I_{ICI}^{odd}, I_{ISI}^{odd} and I_{ICI}^{even} in (18) and (19)
  Perform Interference cancellation, i.e
  $\hat{\mathbf{a}}_n^{even}(i+1) = \hat{\mathbf{a}}_n^{even}(i) - \hat{I}_{ISI}^{even} - \hat{I}_{ICI}^{odd}$, using (18)
  $\hat{\mathbf{a}}_n^{odd}(i+1) = \hat{\mathbf{a}}_n^{odd}(i) - \hat{I}_{ISI}^{odd} - \hat{I}_{ICI}^{even}$, using (19)
  $i = i+1$
end while
Terminate.

IV. Simulation Results

In this section, we present simulation results of the proposed IIC algorithm for FBMC-QAM, FBMC-OQAM and OFDM. For FBMC-QAM and FBMC-OQAM, we employ a PHYDYAS prototype filter with $K = 4$ for the per-subcarrier filtering [8]. We considered the Extended Vehicular A (EVA) and Extended Typical Urban (ETU) channel models as specified by the 3rd Generation Partnership Project (3GPP)

for LTE [19]. The simulation parameters are illustrated in Table I.

Fig. 2 shows the power spectral densities (PSDs) of OFDM, FBMC-OQAM and conventional FBMC-QAM with two prototype filters, and the proposed FBMC-QAM with 512 active subcarriers out of 1024. The proposed FBMC-QAM system shows the same OOB emission performance as FBMC-OQAM. This is mainly due to the better frequency localization of the prototype filter employed for the per subcarrier filtering. The FBMC-QAM system in [15] achieve a slightly worse OOB emission performance compared to OFDM. This is because of the discontinuities in one of the two prototype filters used for the time domain subcarrier filtering.

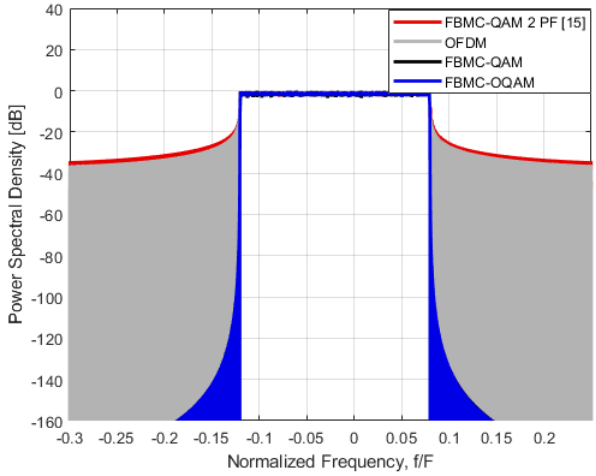

Fig. 2. PSD comparison between OFDM, FBMC-OQAM, FBMC-QAM Orthogonal, and FBMC-QAM Non-orthogonal.

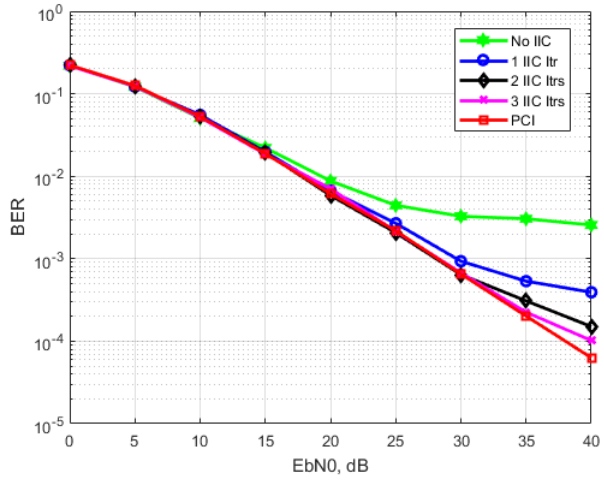

Fig. 3. BER performance of uncoded FBMC-QAM with IIC using 4-QAM over LTE-EVA Channel.

Fig. 3 and Fig. 4 illustrate the BER performance of the proposed IIC FBMC-QAM system in the 3GPP EVA and ETU channel models respectively, when 4-QAM modulated data is transmitted and one-tap frequency domain equalization is performed. We assume that the receiver has perfect channel state information (PCI) and compare our simulation with the results of the PCI interference cancellation. For the PCI implementation, I_{ISI}^{even}, I_{ICI}^{odd}, I_{ISI}^{odd} and I_{ICI}^{even} are calculated directly from the transmitted signal, instead of the estimated signal. It can be seen in these figures that the BER performance is improved after a few IIC iterations. As shown in Fig. 3, the gap from the PCI simulation results is approximately 2 dB at the third iteration, measured at 10^{-4} BER. After 5 iterations, there still remains an error floor under the LTE-ETU channel, though the error floor performance is improved after each iteration, as shown in Fi. 4. This is consistent with the results shown in [13] for both OFDM and FBMC-OQAM.

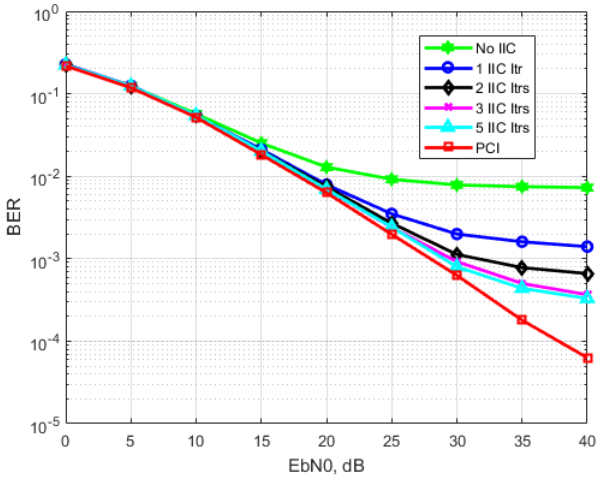

Fig. 4. BER performance of uncoded FBMC-QAM with IIC using 4-QAM over LTE-ETU Channel.

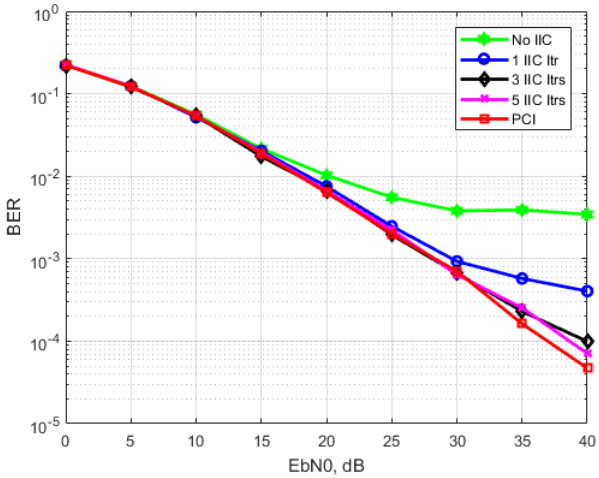

Fig. 5. BER performance of uncoded FBMC-QAM with IIC using 16-QAM over LTE-EVA Channel.

Fig. 5 shows the BER performance of the IIC FBMC-QAM system with 16-QAM and Zero-Forcing (ZF) equalizer

over 3GPP EVA channel. As can be observed from Fig. 5, the error floor is improved significantly after 5 iterations. Measured at 10^{-4}, the gap between 5 iterations of IIC and the PCI simulation results is less than 2 dB. This implies that 5 iterations are enough to obtain an acceptable BER performance and more than 5 iterations will not improve the performance much.

V. Conclusion

In this paper, we proposed the use of iterative interference cancellation to remove the intrinsic interference in FBMC-QAM systems. In order to effectively cancel the effect of interference, we proposed a receiver which separates the received signal into even- and odd-numbered subcarrier components, and uses the decoded even- and odd-numbered subcarrier symbols to iteratively cancel the interference from subsequent symbols.

Numeral simulations show that the IIC algorithm can significantly improve the BER performance of the proposed FBMC-QAM system under different time-varying channels. For example, for the case of 16-QAM in the LTE-EVA channel, it is shown that 5 IIC iterations is able to achieve near optimum BER performance. Also, the OOB emission performance is identical to FBMC-OQAM and is superior to that of both OFDM and conventional FBMC-QAM with two prototype filters. The high spectral efficiency of the proposed FBMC-QAM system make it suitable for applications that require uncoordinated and asynchronous user transmission such as IoT.

References

[1] M. Chen, Y. Miao, Y. Hao, and K. Hwang, "Narrow band internet of things," *IEEE Access*, vol. 5, pp. 20557–20577, 2017.

[2] *Ericsson Mobility Report: Mobile World Congress Edition*, Feb.

[3] C. Sexton, N. J. Kaminski, J. M. Marquez-Barja, N. Marchetti, and L. A. Dasilva, "5G: Adaptable networks enabled by versatile radio access technologies," *IEEE Communications Surveys and Tutorials*, vol. 19, no. 2, pp. 688–720, 2017.

[4] J. G. Andrews, S. Buzzi, W. Choi, S. V. Hanly, A. Lozano, A. C. K. Soong, and J. C. Zhang, "What will 5G be?," *IEEE Journal on Selected Areas in Communication*, vol. 32, pp. 1065–1082, June 2014.

[5] 3GPP, *Study on New Radio Access Technology; Radio Interface Protocol Aspects*, TR 38.804 v14.0.0 (Rel. 14) ed., 2017.

[6] Y. Medjahdi *et al.*, "On the road to 5G: Comparative study of physical layer in MTC context," *IEEE Access*, vol. 5, pp. 26556–26581, Dec. 2017.

[7] A. Sahin, I. Guvenc, and H. Arslan, "A survey on multicarrier communications: Prototype filters, lattice structures, and implementation aspects," *IEEE Commuications Surveys and Tutorials*, vol. 16, no. 3, pp. 1312–1338, 2014.

[8] M. Bellanger, "FBMC physical layer: A primer," tech. rep., 2010.

[9] G. Wunder *et al.*, "5GNOW: Non-orthogonal, asynchronous waveforms for future mobile applications," *IEEE Commun. Mag.*, vol. 52, pp. 97–105, Feb. 2014.

[10] B. Farhang-Boroujeny, "OFDM versus filter bank multicarrier," *IEEE Signal Processing Magazine*, vol. 28, pp. 92–112, May 2011.

[11] D. S. Waldhauser, L. G. Baltar, , and J. A. Nossek, "Adaptive decision feedback equalization for filter bank based multicarrier systems," in *IEEE International Symposium on Circuits and Systems*, pp. 2794–2797, May 2009.

[12] R. Datta, G. Fettweis, Z. Kollar, and P. Horvath, "FBMC and GFDM interference cancellation schemes for flexible digital radio PHY design," in *14th Euromicro Conference on Digital System Design (DSD)*, pp. 335–339, Sept. 2011.

[13] Y. J. Harbi and A. G. Burr, "On ISI and ICI cancellation for FBMC/OQAM system using iterative decoding and ML detection," in *Wireless Communications and Networking Conference (WCNC)*, pp. 1–6, Apr. 2016.

[14] Y. J. Harbi and A. G. Burr, "IIC of the MIMO-FBMC/OQAM system using linear and SIC detection schemes in LTE channel," in *Wireless Communications and Networking Conference (WCNC)*, pp. 1–6, Apr. 2018.

[15] H. Nam, M. Choi, S. Han, C. Kim, S. Choi, , and D. Hong, "A new filter-bank multicarrier system with two prototype filters for QAM symbols transmission and reception," *IEEE Transactions on Wireless Communications*, vol. 15, pp. 5998–6009, Sept. 2016.

[16] B. Kwon, S. Kim, D. Jeon, and S. Lee, "Iterative interference cancellation and channel estimation in evolved multimedia broadcast multicast system using filter-bank multicarrier-quadrature amplitude modulation," *IEEE Transactions on Broadcasting*, vol. 62, pp. 864–875, Dec. 2016.

[17] J. Kim, Y. Park, S. Weon, J. Jeong, S. Choi, and D. Hong, "A new filter-bank multicarrier system: The linearly processed fbmc system," *IEEE Transactions on Wireless Communications*, vol. 17, pp. 4888–4898, July 2018.

[18] M. G. Bellanger, "Specification and design of a prototype filter for filter bank based multicarrier transmission," in *IEEE International Conference on Acoustics, Speech, and Signal Processing*, pp. 2417 – 2420, May 2001.

[19] *Evolved Universal Terrestrial Radio Access (E-UTRA); User Equipment (UE) Radio Transmission and Reception*, TS 136 304, 3GPP TSG RAN ed., 2017.